THE ENTROPY GENERATION IN TRANSIENT THERMAL CONVECTION OVER A FINITE THICKNESS PLATE

Emilia-Cerna MLADIN, Mohammed LACHI**, Mourad REBAY**, Jacques PADET***

*UNIVERSITY POLITEHNICA of Bucharest, e-mail: cerna_mladin@yahoo.fr ,
**UNIVERSITÉ DE REIMS, France, e-mail: mohammed.lachi@univ-reims.fr , mourad.rebay@univ-reims.fr , jacques.padet@univ-reims.fr

***Rezumat.** Autorii au elaborat două modele matematice similare pentru caracterizarea cuplajului termic tranzitoriu în curgeri peste plăci plane de grosime finită. Variațiile temporale sunt induse de modificări tip treaptă în temperatura sau fluxul termic impuse la fața inferioară a plăcii. Soluționarea ecuațiilor de guvernare s-a efectuat prin metoda integrală cu legi de variație a temperaturii în placă și în fluid adaptabile în timp la condițiile limită instantanee. Modelele matematice au fost comparate cu alte soluții matematice raportate în literatură pentru regimuri staționare, rezultând diferențe de maxim. Legile de variație a vitezei și temperaturii au permis calculul entropiei instantanee generate în sistem prin disipare vâscoasă și conducție termică.*

NOMENCLATURE

A $= a/a_p$, fluid and plate diffusivity ratio
C – proportionality factor, eq. (20) ($m^{1/2}$)
E – plate thickness (m)
E_* $= E/C^2$, dimensionless plate thickness
h – convective heat transfer coefficient ($W \cdot m^{-2} \cdot K^{-1}$)
$k_{(p)}$ – fluid/plate thermal conductivity ($W \cdot m^{-1} \cdot K^{-1}$)
q_s – contact surface heat flux ($y = 0$) ($W \cdot m^{-2}$)
q_{s*} – non-dimensional heat flux [eq. (14)]
Pr – fluid Prandtl number
S – entropy ($W \cdot kg^{-1} \cdot K^{-1}$)
T – fluid temperature within the thermal boundary layer (K)
T_p – plate temperature (K)
T_∞ – freestream temperature (K)
T_0 – plate temperature at $y = -E$ (K)
u – fluid velocity in x-direction ($m \cdot s^{-1}$)
U_∞ – freestream velocity ($m \cdot s^{-1}$)
x_* $= x/C^2$ dimensionless coordinate
y_* $= y/E$, dimensionless coordinate

Greek symbols

β $= y/\delta_t$, dimensionless coordinate
δ = hydrodynamic boundary layer thickness (m)
δ_t = thermal boundary layer thickness (m)
η $= y/\delta$, dimensionless coordinate
$\theta = (T - T_\infty)/(T_0 - T_\infty)$
$\theta_s = (T_s - T_\infty)/(T_0 - T_\infty)$
$\theta_p = (T_p - T_\infty)/(T_0 - T_\infty)$

Indices:

ss – steady state
p – relative to the plate
s – relative to the contact surface ($y = 0$)

1. INTRODUCTION

Most of the previous works on heat convection in parallel flows over bodies use various boundary conditions at the contact surface. In all such cases, the plate thermal resistance is not encountered in calculus, although heat transfer may be highly influenced by the impact body geometry and material. Moreover, in practical applications, it is most probably that the boundary conditions are known at the accessible surfaces, i.e. the ones that are not in contact with the fluid flow. Use of common measuring instruments at the contact surface between the fluid and the body would clearly disturb the boundary layers and thus rendering the measurements to be erroneous.

In the present paper, the authors report results that pertain to the dynamics of a parallel laminar flow over a finite thickness flat plate. The plate suddenly comes in contact with a thermostat type body or a constant surface heat flux source, inducing thus temporal variations in the heat flux exchanged with the fluid. Previously developed mathematical models are used for this purpose [1, 2]. Although an extended parameter analysis has been performed, only a few illustrative cases are presented here: water or air flows over plates made of steel or PVC. Nevertheless, the models may be used for any other fluid-solid combination provided that their thermophysical properties still comply with the model assumptions. Figures 1*a* and 1*b* present the schematic of the physical systems considered in this study. An incompressible fluid flows under laminar conditions parallel with a flat plate.

The plate thickness E is assumed much smaller than its length. The fluid has a constant temperature T_∞ and a constant velocity U_∞, as there are no pressure gradients in the freestream. At a certain moment, considered initial, a constant temperature $T_0 \neq T_\infty$ (Fig. 1*a*) or a constant surface heat flux q_{ext} (Fig. 1*b*) is imposed on the back surface of the plate. As the flow is constant, the hydrodynamic boundary layer thickness $\delta(x)$ and velocity profile $u(x, y)$ are also invariable with time.

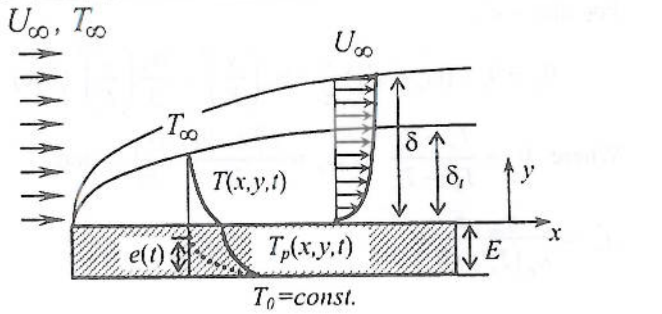

Fig. 1a. Schematic representation of the physical system for $T_0(t \geq 0) = \text{const.}$

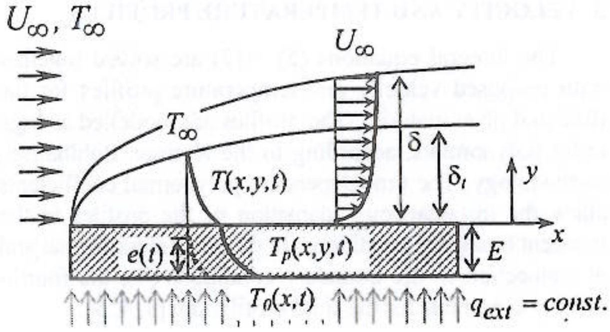

Fig. 1b. Schematic representation of the physical system for $q_{ext}(t \geq 0) = \text{const.}$

When the plate is penetrated by the heat flux (i.e., a temperature gradient reaches the upper surface), the thermal boundary layer grows, having an instantaneous thickness $\delta_t(x,t)$ and an instantaneous temperature profile $T(x,y,t)$. The temperature instantaneous distribution within the impact plate is different for the penetration phase (dotted red line) as opposed to the after-penetration phase (solid red line).

2. CONSERVATION EQUATIONS

Exact analytical solutions are often impossible to find when dealing with transient phenomena. On the other hand, where transient effects can be incorporated with similarity methods for example, the resulting solutions may impose particular relationships between variables. Because of these reasons, the authors have chosen the semi-analytical method of Karman-Pohlhausen. Equations for momentum and energy conservation in their integral and differential forms were used with temporally adaptive profiles for fluid and temperature to obtain governing equations for the thermal boundary layer response [1, 2]. The problem was solved under the following general assumptions: (i) incompressible laminar flow; (ii) constant fluid and solid thermophysical properties; (iii) negligible viscous heating; (iv) negligible body forces in comparison to viscous forces; (v) one-dimensional conduction and no heat sources within the solid; (vi) $\delta_t \leq \delta$. The last assumption restricts the models to fluids with Prandtl numbers greater than about unity. However, related studies indicated reasonable errors for $\Pr \geq 0{,}7$ [3].

Under stationary flow but transient heat transfer conditions, the conservation equations have the differential and integrals forms included in the table below. Within the solid, the one-dimensional transient conduction is modelled by the diffusion equation.

Differential conservation equations

$$\frac{\partial u}{\partial x} + \frac{\partial v}{\partial y} = 0 \tag{1}$$

$$u\frac{\partial u}{\partial x} + v\frac{\partial u}{\partial y} = \nu\frac{\partial^2 u}{\partial y^2} \tag{2}$$

$$\frac{\partial T}{\partial t} + u\frac{\partial T}{\partial x} + v\frac{\partial T}{\partial y} = a\frac{\partial^2 T}{\partial y^2} \tag{3}$$

$$\frac{\partial T_p}{\partial t} = a_p\frac{\partial^2 T_p}{\partial y^2} \tag{4}$$

Integral conservation equations

$$\frac{\partial}{\partial x}\int_0^{\delta} u\left(u - U_\infty\right)dy = -\nu\left.\frac{\partial u}{\partial y}\right|_{y=0} \tag{5}$$

$$\frac{\partial}{\partial t}\int_0^{\delta_t}\left(T - T_\infty\right)dy + \frac{\partial}{\partial x}\int_0^{\delta_t} u\left(T - T_\infty\right)dy = a\left.\frac{\partial T}{\partial y}\right|_{y=0} \tag{6}$$

$$\frac{\partial}{\partial t}\int_{-E}^{-E+e} T_p(y)\,dy - \frac{\partial e}{\partial t}\cdot T_p\left(-E+e\right) = a_p\left.\frac{\partial T_p}{\partial y}\right|_{-E}^{-E+e} \tag{7}$$

The differential equations and physically appropriate matching conditions which must be satisfied by velocity and temperature profiles within the fluid are indicated in Eqs. (8). The plate has a constant and uniform temperature equal to that of the fluid, T_∞, up to the moment considered $t = 0$. After this initial time, the impact plate heat diffusion and matching conditions at the boundaries are given by Eqs. (9).

$$\begin{cases} y \geq \delta \rightarrow u = U_\infty \\ y = 0 \rightarrow u = 0,\ v = 0 \end{cases} \tag{8a}$$

$$\begin{cases} y \geq \delta_t \rightarrow T = T_\infty \\ y = 0 \rightarrow T = T_s;\ \dfrac{\partial T_s}{\partial t} = a\dfrac{\partial^2 T}{\partial y^2} \end{cases} \tag{8b}$$

$$\begin{cases} y = -E \rightarrow T_p = T_0 \ \text{ or } \ q_{ext} = -\lambda_p\dfrac{\partial T_p}{\partial y} \\ y = 0 \rightarrow T_p = T_s;\ \dfrac{\partial T_s}{\partial t} = a_p\dfrac{\partial^2 T_p}{\partial y^2} \end{cases} \tag{9}$$

At the fluid-plate interface, the energy conservation is expressed by the heat flux continuity:

$$q_s = -\lambda\left.\frac{\partial T}{\partial y}\right|_{y=0} = -\lambda_p\left.\frac{\partial T_p}{\partial y}\right|_{y=0} \tag{10}$$

3. VELOCITY AND TEMPERATURE PROFILES

The integral equations (5) – (7) are solved together with proposed velocity and temperature profiles for the fluid and plate material. The profiles are modelled as high order polynomials, according to the Karman-Pohlhausen methodology. The time dependent polynomial coefficients allow the instantaneous adaptation of the profiles to the transient boundary conditions. In dimensionless format and in connection to the boundary conditions (8), the fourth-order polynomials for the fluid profiles are [3, 4, 5]:

$$u_* \equiv \frac{u}{U_\infty} = 2\eta - 2\eta^3 + \eta^4 \ , \ \eta = \frac{y}{\delta} \quad (11)$$

$$\theta \equiv \frac{T - T_\infty}{T_0 - T_\infty} = \theta_S - \left(2\theta_S + \frac{1}{3}\omega\right)\beta + \omega\beta^2 + (2\theta_S - \omega)\beta^3 + \left(-\theta_S + \frac{1}{3}\omega\right)\beta^4 \quad (12)$$

where $\omega \equiv \dfrac{x_* \Pr \Delta^2}{2} \dfrac{\partial \theta_S}{\partial \tau}$.

In the impact plate case, two distinct temporal phases were considered separately: (*i*) the initial phase of plate penetration, treated as conduction through a semi-infinite body with imposed thermal condition at $y = -E$, and (*ii*) after-penetration phase, associated with the thermal boundary layer development within the fluid (see fig. 1). In the first phase, the instantaneous penetration depth is $e(t) \le E$ and the boundary conditions (9) allow the plate temperature profile modelling as a third polynomial [6]. After the heat flux reaches the front plate surface (fig. 1), the boundary conditions al $y = 0$ lead to a different temperature profile inside the plate [7]. The resulting polynomials for the two different boundary conditions at $y = -E$ are separately listed below for the constant temperature case (left) and constant surface heat flux case (right) and $-E \le y \le 0$.

Figures 2a and 2b illustrate selected instantaneous temperature profiles within the impact plate and the fluid, and for both plate penetration and post-penetration phases. As time goes to infinity, the steady-state profiles are asymptotically reached (e.g., a linear plate temperature distribution).

$T_0 =$ const. at $y = -E$ (Fig. 1*a*)

For $0 \le e(t) \le E$:

$$\theta_p^i = 1 - \frac{3}{2}\left(\frac{y + E}{e}\right) + \frac{1}{2}\left(\frac{y + E}{e}\right)^3 \quad (13a)$$

For $e(t) = E$:

$$\theta_p = \theta_s + \left(\theta_s - 1 + \frac{2}{3}\omega_p\right)\frac{y}{E} + \omega_p\left(\frac{y}{E}\right)^2 + \frac{\omega_p}{3}\left(\frac{y}{E}\right)^3 \quad (14a)$$

$q_{ext} =$ const. at $y = -E$ (Fig. 1*b*)

For $0 \le e(t) \le E$:

$$\frac{\theta_p^i}{\overset{\bullet}{q}_{ext}} = \frac{1}{3}\frac{e}{E} - \frac{y}{E} + \frac{E}{e}\left(\frac{y}{E}\right)^2 - \frac{1}{3}\left(\frac{E}{e}\right)^2\left(\frac{y}{E}\right)^3 \quad (13b)$$

For $e(t) = E$:

$$\theta_p = \theta_s + (\omega_p - \overset{\bullet}{q}_{ext})\frac{y}{E} + \omega_p\left(\frac{y}{E}\right)^2 + \frac{\omega_p}{3}\left(\frac{y}{E}\right)^3 \quad (14b)$$

Where $\theta_p \equiv \dfrac{T_p - T_\infty}{T_0^{ss} - T_\infty}$, $\omega_p \equiv \dfrac{E_*^2 A \ \Pr}{2} \dfrac{\partial \theta_s}{\partial \tau}$, and

$$\overset{\bullet}{q}_{ext} \equiv \frac{q_{ext} \cdot E}{\lambda_p \left(T_0^{ss} - T_\infty\right)}$$

4. ENTROPY GENERATION

Fluid flow and heat transfer imply irreversibility by viscous dissipation and thermal diffusion and thus entropy generation in the system. The instantaneous entropy generation rate per unit mass by viscous dissipation within a hydrodynamic boundary layer is given by the following expression [8]:

$$\dot{S}_\nu = \frac{\nu\Phi}{T} = \frac{\nu}{T}\left(\frac{\partial \ u}{\partial \ y}\right)^2 \ [\text{W/kg·K}] \quad (15)$$

The diffusion of thermal energy within a medium represents another source for entropy generation that can be quantified, in case of a thermal boundary layer, by equation (16) [8]:

$$\dot{S}_{\Delta T} = \frac{k}{\rho}\frac{(\nabla T)^2}{T^2} = \frac{k}{\rho}\frac{1}{T^2}\left(\frac{\partial \ T}{\partial \ y}\right)^2 \ [\text{W/kg·K}] \quad (16)$$

Within the fluid, entropy is generated by both viscous dissipation and thermal diffusion. Therefore, the total entropy source is given by the sum of the terms in Eqs. (15) and (16), where velocity and temperature gradients along y-coordinate are deduced from the profiles specified in Eqs. (11) and (12), respectively. In dimensionless form, the entropy source within the fluid is given by Eq. (17).

Within the plate, only entropy generation by thermal diffusion is present. Given the two phases considered during the transient regime, i.e. the penetration phase and post-penetration phase, the temperature gradient along y-coordinate in Eq. (16) is given by Eq. (13) or Eq. (14).

The dimensionless expressions for the entropy sources within the plate are given by Eqs. (18) and (19), with particular forms for the two boundary conditions considered in this study.

The local instantaneous entropy generation within the fluid and the plate is illustrated in Figures 3a and 3b for the cases considered in Figures 2a and 2b. Remarkably, within the fluid the entropy generation by viscous dissipation is a few orders of magnitude lower than entropy generation by thermal dissipation, fact that is supported by the initial assumption regarding the neglecting of the viscous dissipation in the boundary layer governing equations. As the system approaches steady state conditions (i.e., $t \to \infty$), the rate of entropy generation increases within the fluid, while attaining a straight line of positive slope for the plate. Due to the large variations in $\dot{S}_{\Delta T}$, a logarithmic scale was used for its representation.

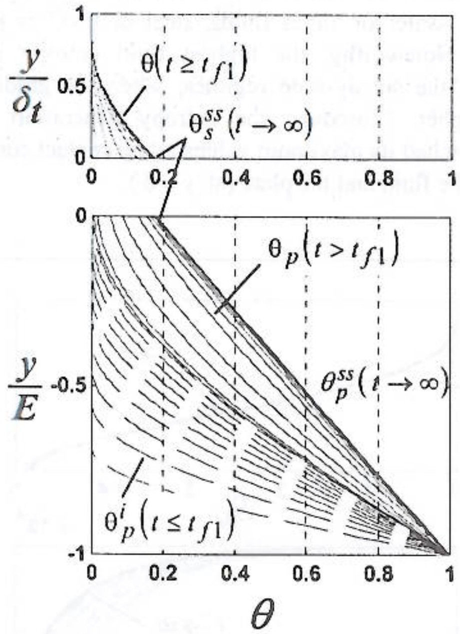

Fig. 2a. The temporal evolution of fluid and plate temperature profiles for air-PVC, $x_* = 300$ and $E_* = 100$ with $T_0(t \geq 0) = \text{const.}$ (Fig. 1a).

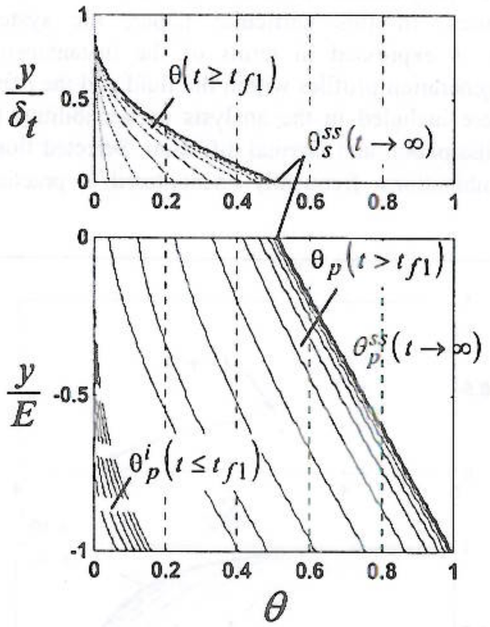

Fig. 2b. The temporal evolution of fluid and plate temperature profiles for water-steel, $x_* = 7000$ and $E_* = 500$ with $q_{ext}(t \geq 0) = \text{const.}$ (Fig. 1b).

$T_0 = \text{const.}$ at $y = -E$ (Fig. 1*a*) $\qquad$ $q_{ext} = \text{const.}$ at $y = -E$ (Fig. 1*b*)

$$\dot{S}_{fluid} = \dot{S}_v + \dot{S}_{\Delta T,fl} \text{ with} \tag{17}$$

$$\dot{S}_v = K_1 \frac{1}{\theta + \theta_{ref}} \left(2 - 6\eta^2 + 4\eta^3\right)^2$$

and

$$\dot{S}_{\Delta T}^{fluid} = K_2 \frac{1}{\Delta^2 \left(\theta + \theta_{ref}\right)^2} \left[-2\theta_s - \frac{\omega}{3} + 2\omega\beta + 3\left(2\theta_s - \omega\right)\beta^2 + 4\left(\frac{\omega}{3} - \theta_s\right)\beta^3\right]^2$$

For $0 \leq e(t) \leq E$:

$$\dot{S}_{\Delta T}^{i,p} = \frac{9K_3 \left(E/e\right)^2}{4\left(\theta_p + \theta_{ref}\right)^2} \left[-1 + \left(\frac{y+E}{e}\right)^2\right]^2 \tag{18a}$$

For $e(t) = E$:

$$\dot{S}_{\Delta T}^{p} = \frac{K_3}{\left(\theta_p + \theta_{ref}\right)^2} \times \left[\theta_s - 1 + \frac{2}{3}\omega_p + 2\omega_p \frac{y}{E} + \omega_p \left(\frac{y}{E}\right)^2\right]^2 \tag{19a}$$

For $0 \leq e(t) \leq E$:

$$\dot{S}_{\Delta T}^{i,p} = \frac{K_3 \cdot \dot{q}_{ext}^{2}}{\left(\theta_p + \theta_{ref}\right)^2} \left[-1 + 2\frac{y+E}{e} - \left(\frac{y+E}{e}\right)^2\right]^2 \tag{18b}$$

For $e(t) = E$:

$$\dot{S}_{\Delta T}^{p} = \frac{K_3}{\left(\theta_p + \theta_{ref}\right)^2} \times \left[\omega_p - \dot{q}_{ext} + 2\omega_p \frac{y}{E} + \omega_p \left(\frac{y}{E}\right)^2\right]^2 \tag{19b}$$

Where the constants are: $K_1 \equiv \dfrac{v^3 \cdot 5.83^4}{C^6 x \left(T_0^{ss} - T_\infty\right)}$, $K_2 \equiv \dfrac{k}{\rho C^2 x}$, $K_3 \equiv \dfrac{k_p}{\rho_p E^2}$, $\theta_{ref} \equiv \dfrac{T_\infty}{T_o^{ss} - T_\infty}$

CONCLUSIONS

Two similar mathematical models were developed to characterize the dynamics of steady parallel flows over a finite thickness plate. Transients are induced by a step change in either the temperature or the heat flux imposed at the back plate surface (i.e. the one that is not in contact with the fluid).

The system governing equations are developed from the energy conservation equations by use of the Karman-Pohlhausen integral approach and time-dependent polynomial profiles for fluid and plate temperatures. In this particular paper, the system dynamics is expressed in terms of the instantaneous entropy generation profiles within the fluid and the plate. There were included in the analysis irreversibilities by viscous dissipation and thermal diffusion. Selected fluid-plate combinations, frequently encountered in practical applications, were considered to illustrate the system dynamics: water or air as fluids, steel or PVC as plate material. Noteworthy, the highest fluid entropy rates related to the steady-state regimes, when the gradients weree higher. Moreover, the entropy generation rate always reached its maximum values at the contact surface between the fluid and the plate (at $y = 0$).

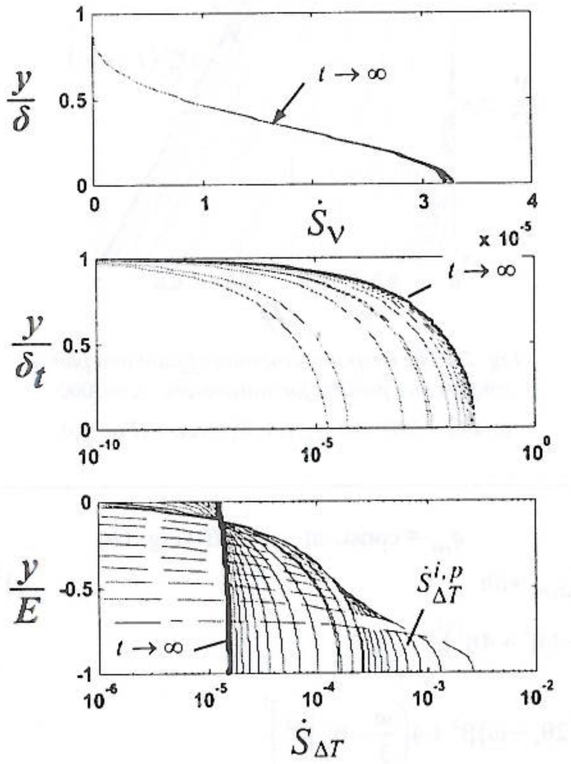

Fig. 3a. The temporal evolution of fluid and plate entropy generation rates for air-PVC, $x_* = 300$, $E_* = 100$ *and* $\theta_{ref} = 20$ *with* $T_0(t \geq 0) = \text{const.}$ *(Fig. 1a).*

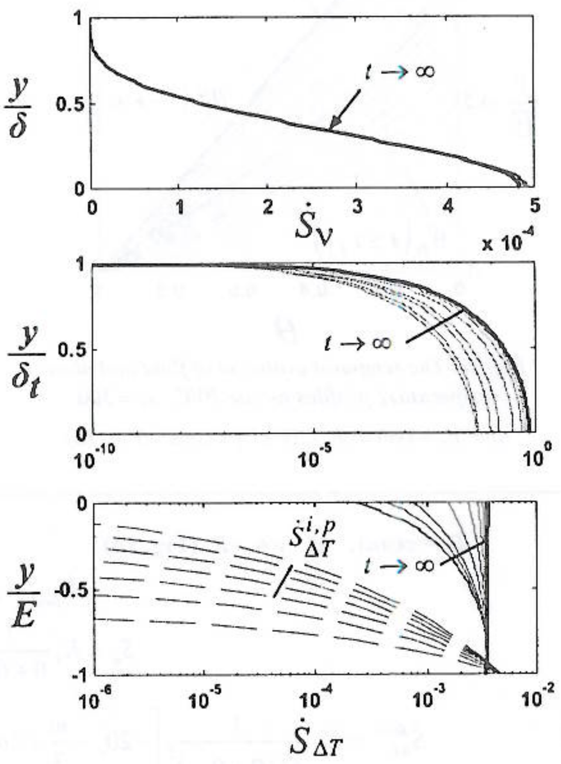

Fig. 3b. The temporal evolution of fluid and plate entropy generation rates for water-steel, $x_* = 7000$, $E_* = 500$ *and* $\theta_{ref} = 20$ *with* $q_{ext}(t \geq 0) = \text{const.}$ *(Fig. 1b).*

REFERENCES

[1] Mladin E.C., Trif A., Lachi M., Padet J., *Couplage convection-conduction en régime transitoire entre un écoulement et une plaque soumise à un échelon de flux thermique*, Travaux du Colloque Franco-Roumain COFRET'02, Bucarest, 25–27 aprilie 2002, pp. 318–326.

[2] Mladin E.C., Radulescu M., Rebay M., Padet J., *Convecție termică tranzitorie în curgeri paralele peste o placă de grosime finită și o față izotermă*, Travaux du Colloque Franco-Roumain COFRET'02, Bucarest, 25–27 aprilie 2002, pp. 326–334.

[3] Mladin E.C., Padet J., *Unsteady planar stagnation flow on a heated plat*", International Journal of Thermal Sciences (Révue Génerale de Thermique), Vol. 40, No. 7, pp. 638–648, 2001.

[4] Succec J., *Heat Transfer*, WM.C. Brown Publishers, Iowa, 1985.

[5] Leca A., Mladin E.C., Stan M., *Transfer de căldură și masă*, Editura Tehnică, București, 1998.

[6] Özişik M.N., *Heat Conduction*, 2nd Edition, John Wiley &Sons, Inc., New York, 1993.

[7] Mladin E.C., Lachi M., Padet J, *Transfert de chaleur couplé conduction-convection en régime instationnaire, induit par une temperature imposée sur une plaque d'épaisseur finie*, Congres Francais de Thermique, SFT Nantes, 29-31 Mai 2001, pp. 87–92.

[8] Bejan A., *Entropy generation through heat and fluid flow*, John Wiley &Sons, New York, 1982.